Hindawi
Mathematical Problems in Engineering
Volume 2018, Article ID 6128368, 10 pages
https://doi.org/10.1155/2018/6128368

*Research Article*

# Understanding Rockburst-Generating Behaviors and Associated Seismicity by Using a Spatial Calculation Methodology with an Energy Density Index

**Guifeng Wang,[1,2] Xiaoyuan Yuan,[1] Siyuan Gong,[1] Linming Dou,[1] Wu Cai,[1] and Chaojun Fan[2]**

[1] *State Key Laboratory of Coal Resources and Safe Mining, School of Mines, China University of Mining and Technology, Xuzhou 221116, China*
[2] *Department of Energy and Mineral Engineering, G3 Center and Energy Institute, The Pennsylvania State University, University Park, PA 16802, USA*

Correspondence should be addressed to Siyuan Gong; wgfskl1982@gmail.com and Linming Dou; psuchildren@163.com

Received 15 August 2018; Accepted 2 October 2018; Published 13 November 2018

Academic Editor: Francisco J. Montáns



Rockbursts have become one of the most severe risks in underground coal mining. A proper understanding of the relationship between the spatial activities of mining-induced tremors and the occurrence of rockbursts can provide effective insight into the evaluation of rockburst hazard as well as revealing their causes. A methodology for spatially calculating the seismicity involving the use of an energy density index was developed to identify the evolution of mining-induced tremors over time. The results showed that numerous tremors occurred during the excavation and mining periods, and those tremors were distributed in a spatially complicated fashion, and it was difficult to identify their evolution trends over time and assess the rockburst hazard. However, energy density clouds had obvious distinguishable trends that presented nucleation characteristics and followed obvious extension around the nucleuses until strong tremors took place nearby. Velocity tomograms indicated that evolution of energy density clouds was the response to the rising stress concentration in some local areas before the rockburst. Then the rockburst-generating journey was inferred; that is, the jump of stress in local areas of coal-rock masses results in the clustering and nucleation of microfractures firstly, and then as the microfractures developed, macrofractures appeared, bringing strong tremors which triggered the rockburst.

## 1. Introduction

Microseismic (MS) monitoring is an important means for investigating the occurrence law of rockbursts in underground engineering. The occurrence of rockbursts is actually the development process of microfractures in coal-rock masses. The tremors detected by MS system reflect the locations and energy release of microfractures. Moreover, the spatial migration and clustering law of tremors over time provide useful insight into the development of microfractures in coal-rock masses before the occurrence of rockbursts. A majority of mining-induced tremors take place during the excavation and mining periods. Previous studies have revealed that rockburst locations are significantly correlated with the spatial activities of mining-induced tremors over time. The mining-induced tremors often change in time from discrete to relatively concentrated distribution before rockbursts [1–3].

As the mining depths grow, rockbursts occur frequently in coal mines of China. At present, more than 170 coal mines in China have suffered from rockbursts. A proper understanding of the relationship between the activities of mining-induced tremors and the occurrence of rockbursts can provide effective insight into the evaluation of rockburst hazard as well as revealing their causes. Current research mainly includes fractal theory [4–6], cluster analysis [2], etc., which have received good results. However, due to the diverse geological conditions, complex mining environments, and changing mining-induced stress, the evolution of microfractures in coal-rock masses is extremely complex

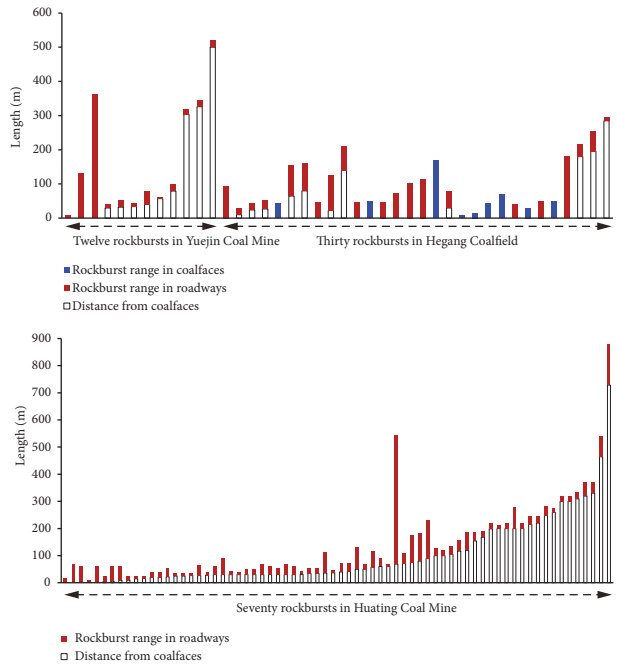


Figure 1: Statistics of locations and damage ranges caused to roadways and coalfaces by rockbursts.

during mining. The mining-induced tremors therefore have rather complex spatial distribution characteristics as well. For this reason, it is hard to directly obtain the spatial evolution law of tremors over time [5, 7]. Detecting hazardous areas and judging its present hazardous state are critical for manual intervention in advance to prevent the rockburst. However, effective means to detect potential rockburst locations and assess the rockburst hazard still remain in the exploration and development because of the complexity of the rockburst-generating behavior and the difficulty of precisely identifying the evolution law of mining-induced tremors in a complicated rock mass fabric.

In this work, occurrence characteristics of rockbursts and the difficulties for identifying the evolution law of associated spatial seismicity were analyzed. A methodology for spatially calculating the seismicity involving the use of an energy density index was developed to identify the evolution of mining tremors over time. Case studies were taken to investigate the spatial activity characteristics of mining-induced tremors before the occurrence of rockbursts. Then, the rockburst-generating journey was inferred by combining further stress detection by the seismic velocity tomography. This study may eventually lead to a methodology for identifying the potential rockburst location, which is critical for manual intervention in advance to prevent the rockburst; thus it would provide a significant advance in the enhancement of safety in coal mines.

## 2. Field Investigations

Figure 1 shows statistics of locations and damage ranges caused to roadways and coalfaces by rockbursts. It can be seen that rockbursts all took place in local regions which might have high stress concentration and damaged sections of tens or hundreds of meters long. Rockbursts occurred mostly in the tailgate and headgate, and their locations often had a distance from the coalface. The distance defined from the coalface to the nearest end of the rockburst area varies greatly from zero to several hundred meters. The stress plays an important role in rockburst occurrence [8]. A rockburst is more likely to occur in areas with high stress concentration. For example, in some local regions of a working face where there are folds, coal pillars, and suddenly changing thickness or inclination of coal seam, coal-rock masses are likely to store great quantities of elastic energy. When the coalface is advanced to these regions, the mining-induced stress is superposed on the tectonic stress or the stress imposed by coal pillars, etc.; then rockbursts are prone to occur in these regions.

Spatial rockburst locations and damage characteristics of rockbursts were shown in Figure 2. The rockburst on 15 March 2013 in Junde Coal Mine, Hegang City, caused damage to all of the tailgate, headgate, and coalface, simultaneously (Figure 2(a)). Both the tailgate and headgate were closed and 25 miners were trapped. Rockbursts have resulted in floor heave, coal wall movement, wire mesh tearing, anchor bolt and U-type steel support failure, coal cutter flying, etc. As shown in Figure 2(b), two rockbursts occurred at Xing'an Coal Mine (Heilongjiang Province, China) during mining in the syncline region. The rockburst on 26 June 2012 occurred in tailgate near the coalface, while the other rockburst on 15 October 2012, which left a 104-m-length of roadway damaged, was the first one to take place in the haulage roadway close to the solid coal. It was also reported that the rockburst on 15 September 2016 occurred behind the driving coalface in an open-off cut of Junde Coal Mine (Figure 2(c)). At that time, the rockburst caused the closure of the upper section of the open-off cut and five miners were trapped near the driving coalface.

With the extraction of underground coal masses and the movement of rock stratum, stress around the stope constantly changes during the excavation and mining periods. The development of microfractures is the response of coal-rock masses to the stress changes, and the evolution of tremors corresponds to the development of microfractures. In situ MS monitoring is a very effective method to reflect the rockburst-generating behaviors. The more concentrated the tremors in a local area, the larger the probability for the formation of macrofractures due to the further extension and connection of microfractures in coal-rock masses, and the larger the occurrence of rockbursts [1, 9, 10].

Figure 3 shows the spatial distribution of mining-induced tremors before the rockburst on 15 March 2013 in Junde Coal Mine. As the seismicity corresponds to the occurrence and development process of microcracks in coal-rock masses, the spatial distribution of tremors was extremely complex and evolved in a nonlinear manner over time [1, 3, 11]. It was difficult to intuitively observe the evolution trend over time and extract the rockburst precursors from these spatial distribution maps to assess the rockburst hazard, until a strong tremor of $3.09 \times 10^6$ J took

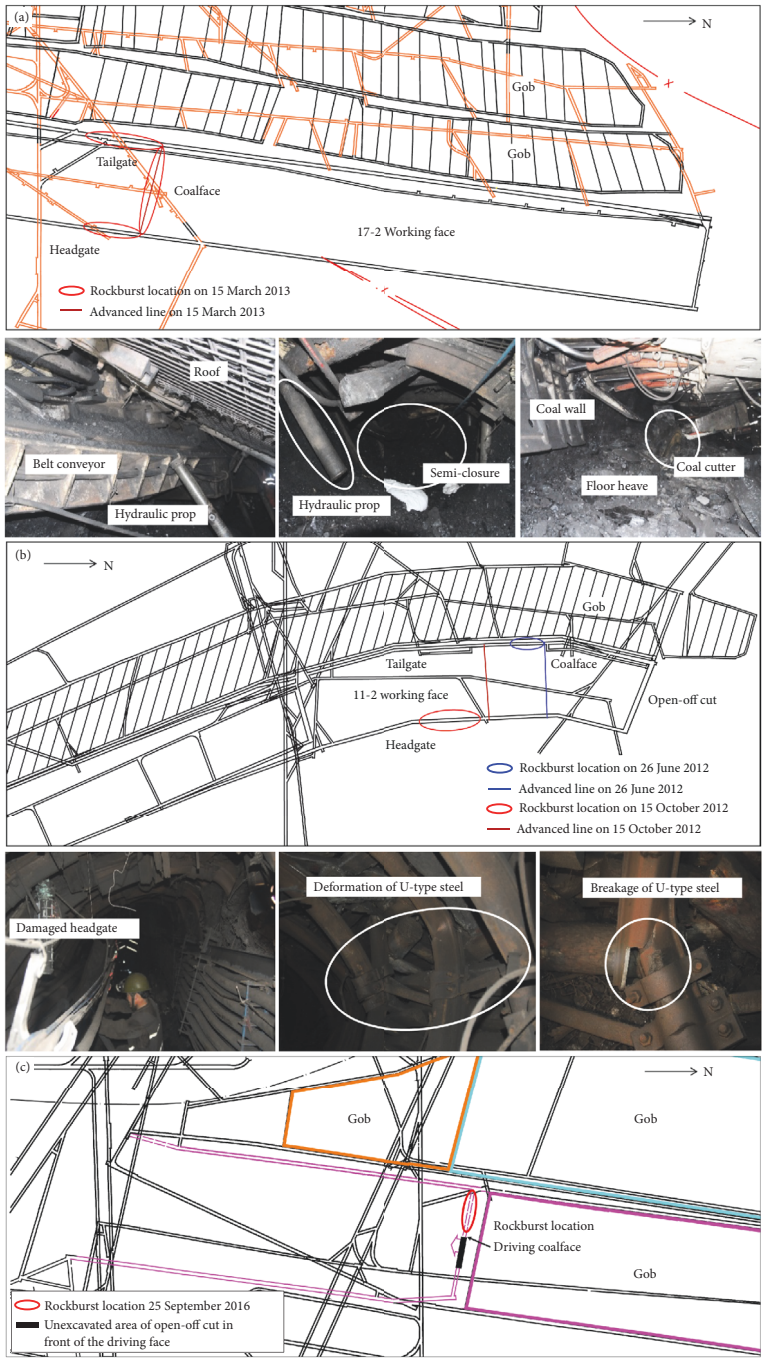


Figure 2: Spatial rockburst locations and damage characteristics of rockbursts in Junde Coal Mine on 15 March, 2013 (a), Xing'an Coal Mine (b), and Junde Coal Mine on 25 September, 2016 (c), respectively.

place and triggered the violent rockburst on 15 March 2013.

## 3. Spatial Calculation Methodology

As mentioned above, the generating process of rockbursts could not be inferred by those spatial distribution maps. In this study, we address this problem by developing a spatial calculation methodology with an energy density index. As shown in (1), the locations, energy, and distances of tremors and time parameter were integrated together to establish the spatial energy density index. The flow chart for the spatial calculation methodology is expressed in Figure 4.

$$\rho_j = \lg\left(\frac{\sum_{t_i \in P} \sqrt{E_{t_i}}}{S_j}\right) \tag{1}$$

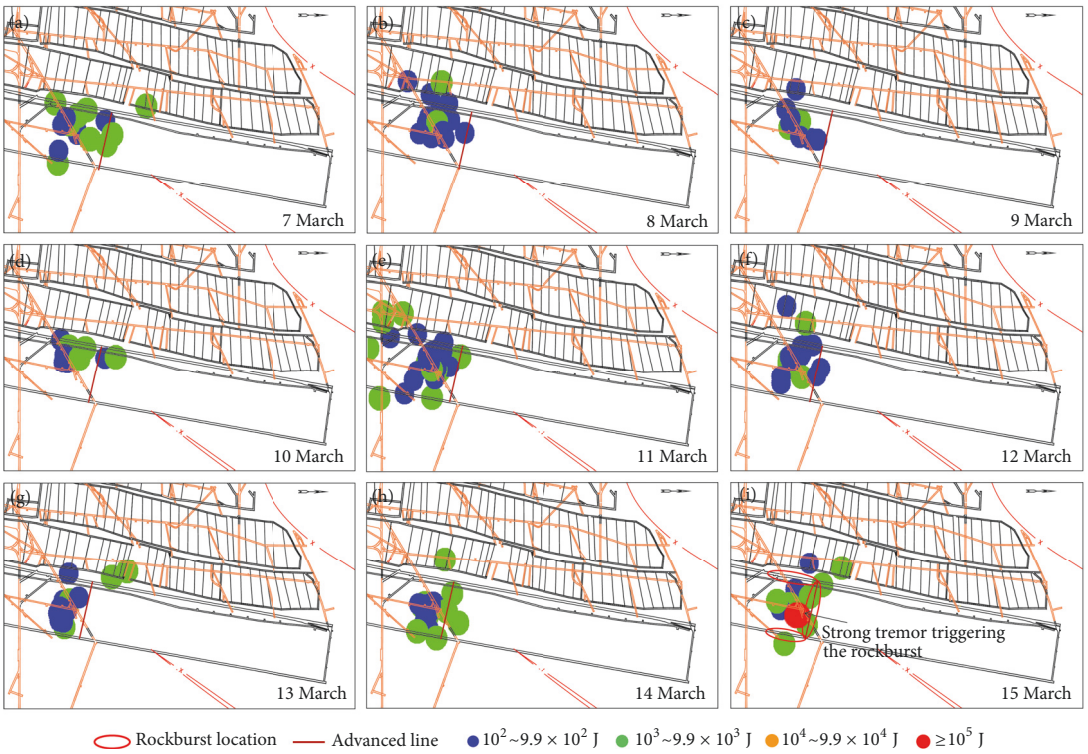


Figure 3: Spatial distribution maps of tremors before the rockburst in Junde Coal Mine (March 7–15, 2013).

The stope was divided into many rectangular grids for the calculation of seismic data based on the spatially smoothed seismicity model, which adopted spatial points of seismic events to calculate the rockburst hazard [12]. As the function of (1) shows, $\rho_j$ was the energy density index of a node belonging to the $j$-th statistical grid, $\lg(\sqrt{J}/m^2)$; $E_{t_i}$ represented the energy of tremors, which were located around the note of $j$-th region and were selected to compute the energy density index as the function of (1), during the statistical time windows denoted by $P$ (days), $J$; and $S_j$ denotes the area of the statistical grid ($m^2$). Thus, a daily energy density contour map was obtained. The spatial energy density index mainly characterized the clustering and development process of tremors in the perspective of energy. The index can not only reflect the locations and energy release of microfractures, but also characterize the clustering and development process of microfractures over time. The area with high energy density is the place where the microfractures concentrate and the coal-rock masses are severely damaged.

## 4. Rockburst-Generating Behaviors

Geological and mining conditions greatly influence the evolution of microfractures in coal-rock masses. Thus the tremors have different spatial activity characteristics, and rockbursts also exhibit varying occurrence law. The spatial activities of tremors before the rockburst (Figure 2(a)) on 15 March 2013 in Junde Coal Mine were analyzed using the spatial calculation methodology. As shown in Figure 5, a very clear activity law of tremors was obtained from the evolution of energy density clouds. From 7 to 9 March, it seemed more obvious that the nucleus of energy density clouds had formed. From 10 to 14 March, the energy density clouds expanded quickly around the nucleation area, with a gradual increase in the intensity and distribution area. Until 15 March in Figure 5(i), a strong tremor of $3.09 \times 10^6$ J occurred in the vicinity of the energy density cloud and triggered the rockburst. As tremors truly reflect the ruptures of rock masses, it can be inferred that microfractures gradually concentrated and changed from the original disordered and scattered distribution to the ordered distribution [13, 14]. The nucleation and strengthening of the energy density clouds were the precursor of the rockburst. Therefore, the area of high energy density clouds could be used to identify the potential rockburst locations, and the growing strength thereof was beneficial for assessing the hazardous state in time.

Figure 6 shows the spatial seismicity and energy density clouds before the rockburst on 15 October 2012 in Xing'an Coal Mine (Figure 2(b)). The amount of tremors increased approximately firstly from October 8 to 13 and then decreased on October 14 before the occurrence of the rockburst. However, in energy density cloud maps, nucleation areas began to appear in the synclinal region (Region A) on 8 October 2012, indicating that microfractures started to concentrate in local areas. Then in the following two days, the nucleation phenomenon of the energy density clouds became more obvious. From 11 to 14 October, the energy density clouds extended around the nucleus with a dramatical augment

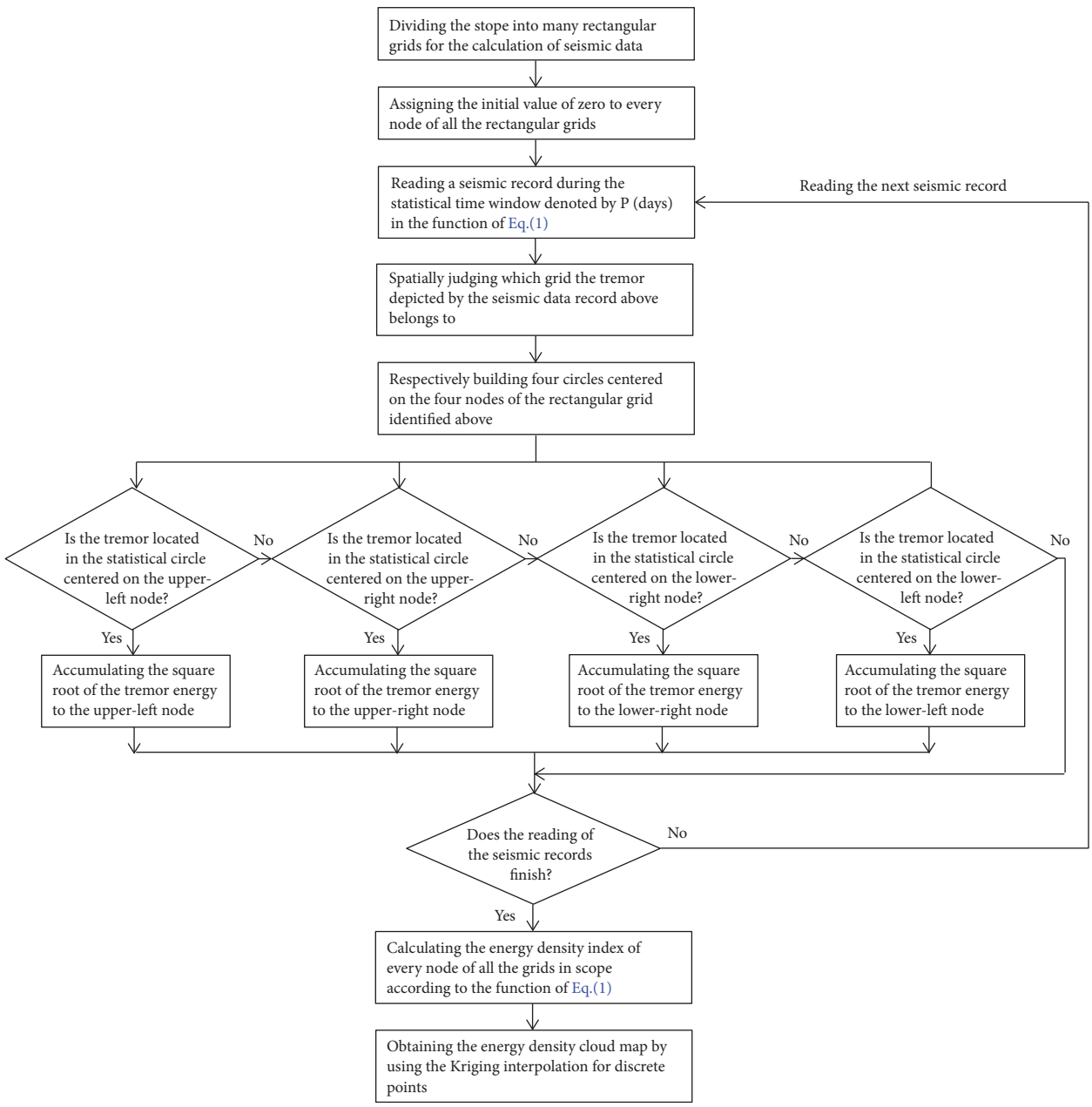


Figure 4: Flow chart for the spatial calculation methodology.

in the intensity. Then, as shown in Figure 6(i), two strong tremors took place in succession at the synclinal axis. The first strong tremor of $1.29 \times 10^5$ J only induced obvious shocks, while the second one of $3.02 \times 10^5$ J triggered a violent rockburst. The area with high energy density clouds was consistent with the rockburst location.

As Figures 5 and 6 show, strong tremors which triggered the rockbursts both occurred near the edges of the energy density clouds. The phenomenon is frequently seen in the failure of rocks in laboratory-scale AE experiments. That is, high energy AE events mainly happen in the edges of the microfracture concentration regions, instead of at the center thereof [2, 15, 16]. This was probably because numerous microcracking events had occurred in the nucleation areas, and it caused stress relaxation and stress transfer to the edges of high energy density clouds, which would be subjected to a high stress concentration and stored huge releasable energy. As microfractures developed, the energy homeostasis in the edges was disrupted and the energy stored in the coal-rock masses was suddenly released, causing strong tremors which triggered rockbursts.

While tunneling the open-off cut of a working face on 25 September 2016 in Junde Coal Mine, a severe rockburst occurred causing the closure of the open-off cut (Figure 2(c)). The spatial seismicity and energy density clouds before the rockburst are shown in Figure 7. As demonstrated in

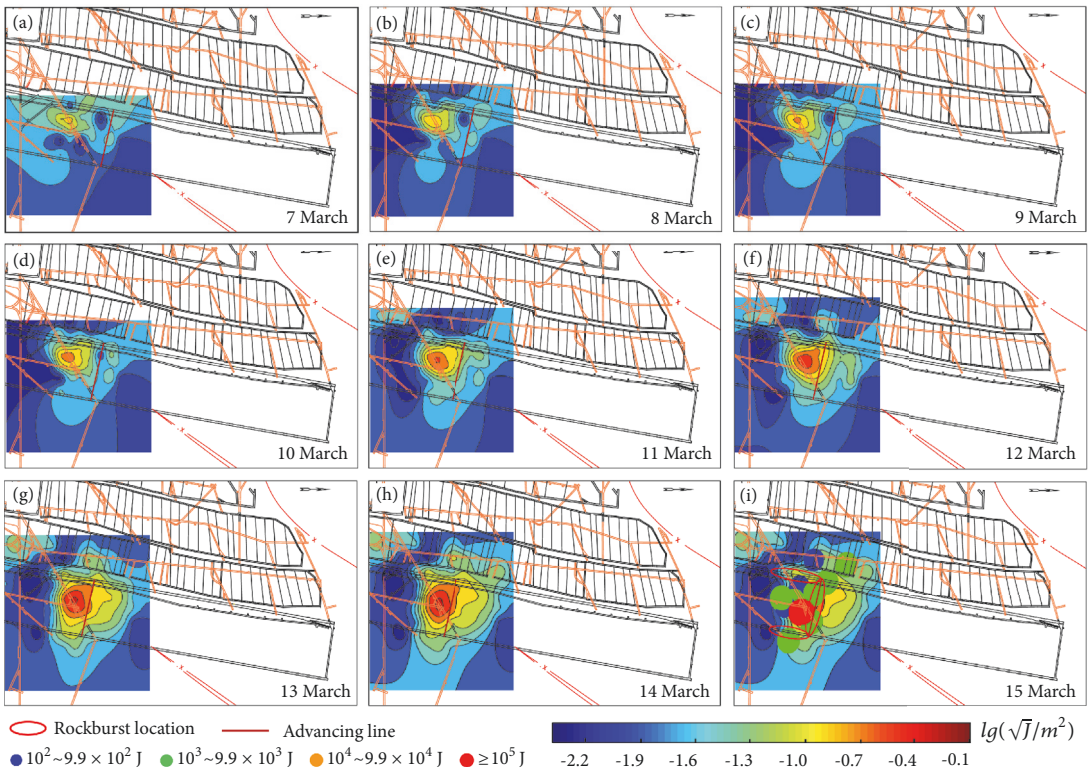


Figure 5: Energy density clouds of tremors before the rockburst in Junde Coal Mine (March 7–15, 2013).

Figure 2(c), there was a coal pillar of 10-15 m wide between the open-off cut and three gobs around the working face. Miners tunneled from the upper part of the open-off cut using a tunnel-boring machine and the rockburst took place when the open-off cut was about to be cut through, leaving 22 m long unexcavated open-off cut. The residual lengths of unexcavated open-off cut in tunneling were designated by black thick lines in Figure 7. According to the pictures of energy density clouds, it can be clearly seen that the high energy density cloud began to appear in region B on 18 September 2012. Then, region B became the nucleus for the expansion of the energy density clouds. From 19 to 24 September 2012, the expansion speeded up leading to the increases in the area and strength of the high energy density clouds. On 25 September 2012, a strong tremor of $8.82 \times 10^4$ J took place in the vicinity of the energy density clouds, and then the rockburst took place.

## 5. Stress Changes

The seismicity is closely associated with stress changes during the excavation and mining periods. Seismic velocity tomography has been used to detect stress changes. It is found that high-velocity distribution is well consistent with these areas under high stress concentration where tremors are prone to concentrate in the further excavation and mining [17–19]. Figure 8 shows the SOS MS system (a) and schematic map of seismic velocity tomography (b). The seismic wave induced by a mining tremor travels to MS probes located around the stope, respectively, and several traveling rays between the mining tremor and the MS probes were formed. Thus tremors occurring during a statistical period have numerous traveling rays. The seismic wave has varying traveling velocity in different regions of coal-rock masses which can be divided into a lot of 3D grids. The seismic velocity of $V(x, y, z)$ in every 3D grid can be inversed by calculating the traveling parameters of rays, involving locations of MS probes and tremors, and the first-break time of seismic waves. The mathematical model of seismic velocity tomography is as follows [20].

$$V = \frac{L}{T} \longrightarrow VT = L \tag{2}$$

$$T_i = \int_{L_i} \frac{dL}{V(x, y, z)} \quad (i = 1, \cdots, N) \tag{3}$$

$$T_i = \sum_{j=1}^{M} \frac{d_{ij}}{V(x, y, z)} \quad (i = 1, \cdots, N) \tag{4}$$

$L_i$ and $T_i$ denote the travel distance and time of *i-th* seismic wave induced by the mining tremor, respectively. $d_{ij}$ is the distance of the *i-th* seismic wave ray crossing the *j*-th grid; $N$ is the total number of rays; and $M$ is the number of 3D grids.

Then a matrix is formed as (4) and the algorithm of simultaneous iterative reconstructive is used to process

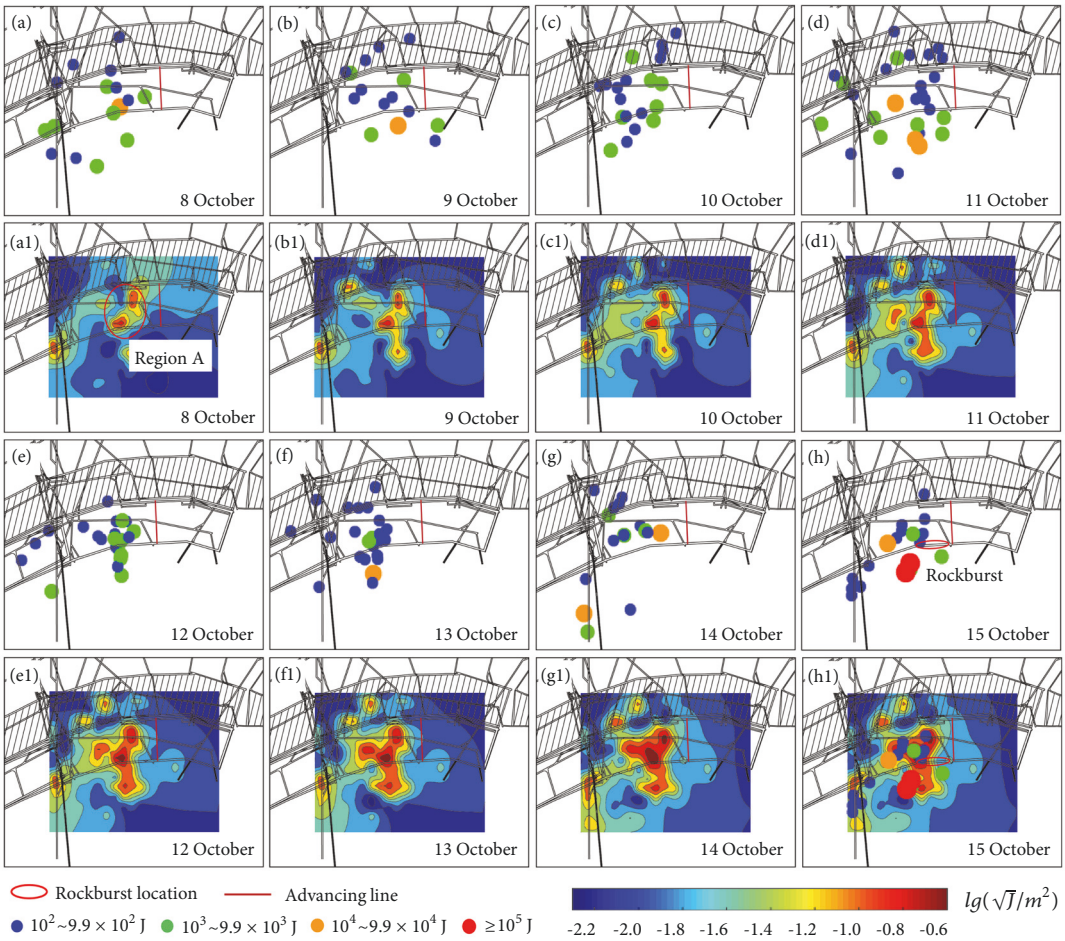


Figure 6: Spatial seismicity and energy density clouds before the syncline-induced rockburst in Xing'an Coal Mine (October 8–15, 2012).

the seismic data [19, 20]. Velocity tomograms before the rockburst on September 25, 2016, in Junde Coal Mine are displayed in Figure 9. The high-velocity regions with red color correspond to areas under high stress concentration. As shown in Figure 9(a), region B at the upper part of the open-off cut began to appear as a high-velocity region, which indicated that region B presented stress concentration. From 16 to 21 September 2016, the wave velocity in region B increased and the distribution area enlarged gradually, which implied that the stress in the region augmented. On 22 September 2016, the wave velocity in region B tended to decline, because the large number of microfractures in region B led to the decrease of wave velocity thereof.

By combining Figures 7 and 9, it can be seen that the high-velocity region was in accord with the area covered by the high energy density clouds. However, the high stress feature in region B began to appear on September 14, 2016, earlier than the emergence of energy density clouds, which indicated that the occurrence of tremors was the response to the rising stress concentration. Meanwhile, as shown above, mining-induced tremors with small energy occurred at first before strong tremors, and according to the evolution of energy density clouds and the stress changes, spatial generating journey of the rockburst could be deduced. That was, the excavation and mining constantly resulted in the stress adjustment, during which stress frequently jumped in local regions. Then the microfractures clustered, the phenomenon of localized nucleation occurred, and the occurrence of microfractures changed from a disordered state to an ordered one. With the increase of local stress and the development of microfractures, macrofractures appeared finally, triggering strong tremors and the following rockbursts.

Studies found that rock ruptures at different scales develop from localized deformation resulting from localized stress and inherent defects in coal-rock masses [16, 21, 22]. The ruptures of small rock samples in laboratories also develop from uniform deformation to localized deformation and finally sudden rupture. This is a significant geological phenomenon before the occurrence of main ruptures and is closely related to the failure of underground rock masses. Scholars have studied the feasibility for predicting the failure of rock masses from the perspective of localized deformation. In their research, the development process of rockbursts was divided into four phases, namely, the stress adjustment, the energy accumulation, the nucleation and expansion of fractures, and the ejection of surrounding rock [23–25].

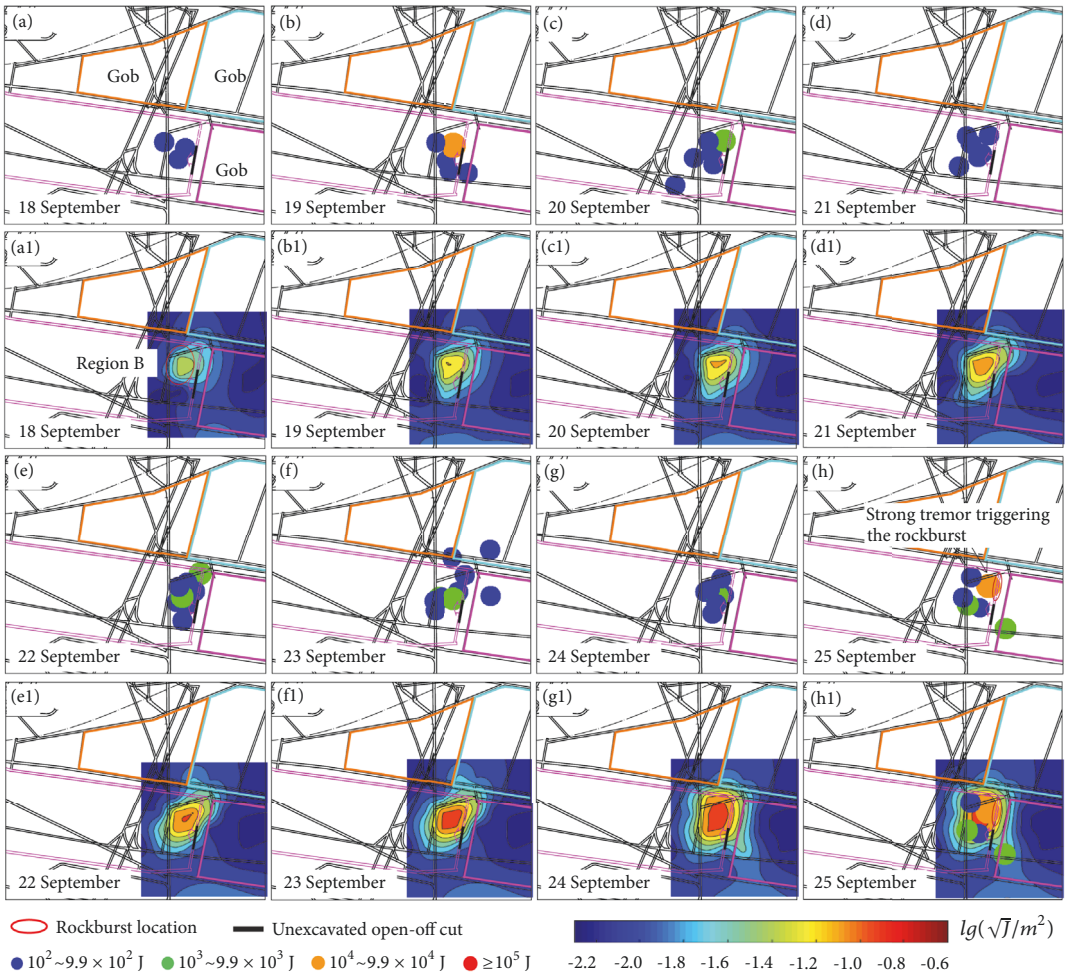


Figure 7: Spatial seismicity and energy density clouds before the tunneling-induced rockburst in Junde Coal Mine (September 18–25, 2016).

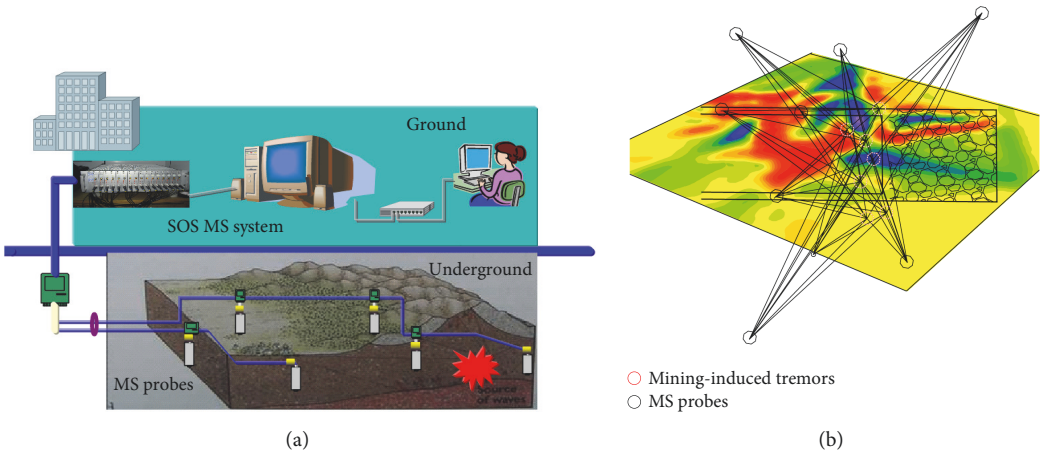


Figure 8: SOS MS system (a) and schematic map of seismic velocity tomography (b).

## 6. Conclusions

The research involved a better understanding of rockburst-generating behaviors and associated seismicity using a spatial calculation methodology with an energy density index. The following conclusions were obtained:

(1) Mining tremors were located in a spatially complicated fashion, and it was hard to obtain their evolution trend over time. The energy density clouds had obvious nucleation characteristics and then extended around the nucleuses until strong tremors took place and triggered the rockburst.

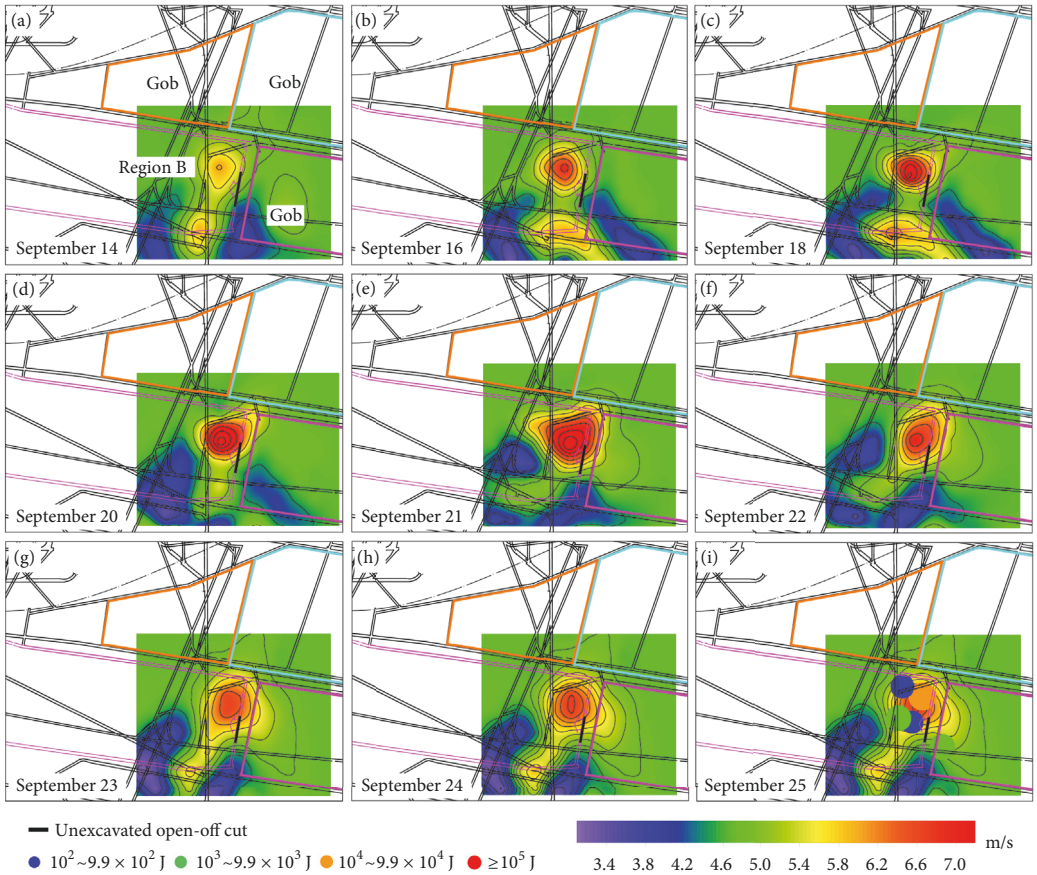


Figure 9: Velocity tomograms before the tunneling-induced rockburst in Junde Coal Mine (September 14–25, 2016).

Areas of energy density clouds were spatially coherent with locations of later rockbursts.

(2) Velocity tomograms indicated that evolution of energy density clouds was the response to the rising stress concentration in some local areas before the rockburst. The rockburst-generating journey was inferred; that is, the stress jumped in local areas, leading to the clustering and nucleation of microfractures, and then as the microfractures developed, macrofractures appeared, bringing strong tremors which triggered the rockburst.

## Data Availability

The MS data used to upport the findings of this study are available from the corresponding author upon request.

## Conflicts of Interest

The authors declare that they have no conflicts of interest.

## Acknowledgments

This work was supported by the Fundamental Research Funds for the Central Universities [grant number 2017QNA27]; the Academic Programme for Development of Jiangsu Higher Education Institutions in China [grant number SZBF2011-6-B35]; the State Key Laboratory of Coal Resources and Safe Mining, CUMT [grant number SKLCRSM16X05]; the National Natural Science Foundation of China [grant number 51504248, 51604270]; and the State Key Research Development Programme of China [grant No. 2016YFC0801403].

## References

[1] B. Brady and F. Leighton, "Seismicity anomaly prior to a moderate rock burst: A case study," *International Journal of Rock Mechanics and Mining Sciences & Geomechanics Abstracts*, vol. 14, no. 3, pp. 127–132, 1977.

[2] A. Leśniak and Z. Isakow, "Space-time clustering of seismic events and hazard assessment in the Zabrze-Bielszowice coal mine, Poland," *International Journal of Rock Mechanics and Mining Sciences*, vol. 46, no. 5, pp. 918–928, 2009.

[3] A.-Y. Cao, L.-M. Dou, C.-B. Wang, X.-X. Yao, J.-Y. Dong, and Y. Gu, "Microseismic precursory characteristics of rock burst hazard in mining areas near a large residual coal pillar: a case study from xuzhuang coal mine, xuzhou, China," *Rock Mechanics and Rock Engineering*, vol. 49, no. 11, pp. 1–16, 2016.

[4] Y. Kagan and L. Knopoff, "Statistical study of the occurrence of shallow earthquakes," *The Geophysical Journal of the Royal Astronomical Society*, vol. 55, no. 1, pp. 67–86, 1978.

[5] X.-T. Feng, Y. Yu, G.-L. Feng, Y.-X. Xiao, B.-R. Chen, and Q. Jiang, "Fractal behaviour of the microseismic energy associated

with immediate rockbursts in deep, hard rock tunnels," *Tunnelling and Underground Space Technology*, vol. 51, pp. 98–107, 2016.

[6] M.-X. Li, Y.-H. Song, and G. Zhang, "Study on the fractal characteristics of rock in the prediction of rockburst," *RSC Advances*, vol. 7, no. 68, pp. 43073–43082, 2017.

[7] Z.-L. Li, L.-M. Dou, G.-F. Wang, W. Cai, J. He, and Y.-L. Ding, "Risk evaluation of rock burst through theory of static and dynamic stresses superposition," *Journal of Central South University of Technology*, vol. 22, no. 2, pp. 676–683, 2015.

[8] W. D. Ortlepp and T. R. Stacey, "Rockburst mechanisms in tunnels and shafts," *Tunnelling and Underground Space Technology*, vol. 9, no. 1, pp. 59–65, 1994.

[9] M. Alber, R. Fritschen, M. Bischoff, and T. Meier, "Rock mechanical investigations of seismic events in a deep longwall coal mine," *International Journal of Rock Mechanics and Mining Sciences*, vol. 46, no. 2, pp. 408–420, 2009.

[10] D. Song, E. Wang, Z. Li, L. Qiu, and Z. Xu, "EMR: An effective method for monitoring and warning of rock burst hazard," *Geomechanics and Engineering*, vol. 12, no. 1, pp. 53–69, 2017.

[11] R. Patyńska, "The consequences of rock burst hazard for Silesian Companies in Poland," *Acta Geodynamica et Geomaterialia*, vol. 10, no. 2, pp. 227–235, 2013.

[12] A. Frankel, "Mapping seismic hazard in the central and eastern United States," *Seismological Research Letters*, vol. 66, no. 4, pp. 8–21, 1995.

[13] B. Orlecka-Sikora, S. Lasocki, G. Lizurek, and Ł. Rudziński, "Response of seismic activity in mines to the stress changes due to mining induced strong seismic events," *International Journal of Rock Mechanics and Mining Sciences*, vol. 53, pp. 151–158, 2012.

[14] J. Kornowski and J. Kurzeja, "Prediction of rockburst probability given seismic energy and factors defined by the expert method of hazard evaluation (MRG)," *Acta Geophysica*, vol. 60, no. 2, pp. 472–486, 2012.

[15] C. Srinivasan, S. K. Arora, and R. K. Yaji, "Use of mining and seismological parameters as premonitors of rockbursts," *International Journal of Rock Mechanics and Mining Sciences*, vol. 34, no. 6, pp. 1001–1008, 1997.

[16] C. Khazaei, J. Hazzard, and R. Chalaturnyk, "Damage quantification of intact rocks using acoustic emission energies recorded during uniaxial compression test and discrete element modeling," *Computers & Geosciences*, vol. 67, no. 6, pp. 94–102, 2015.

[17] K. Luxbacher, E. Westman, P. Swanson, and M. Karfakis, "Three-dimensional time-lapse velocity tomography of an underground longwall panel," *International Journal of Rock Mechanics and Mining Sciences*, vol. 45, no. 4, pp. 478–485, 2008.

[18] N. Hosseini, K. Oraee, K. Shahriar, and K. Goshtasbi, "Studying the stress redistribution around the longwall mining panel using passive seismic velocity tomography and geostatistical estimation," *Arabian Journal of Geosciences*, vol. 6, no. 5, pp. 1407–1416, 2013.

[19] L.-M. Dou, Z.-L. Mu, Z.-L. Li, A.-Y. Cao, and S.-Y. Gong, "Research progress of monitoring, forecasting, and prevention of rockburst in underground coal mining in China," *International Journal of Coal Science & Technology*, vol. 1, no. 3, pp. 278–288, 2014.

[20] W. Cai, L. Dou, S. Gong, Z. Li, and S. Yuan, "Quantitative analysis of seismic velocity tomography in rock burst hazard assessment," *Natural Hazards*, vol. 75, no. 3, pp. 2453–2465, 2014.

[21] V. L. Shkuratnik, Y. L. Filimonov, and S. V. Kuchurin, "Regularities of acoustic emission in coal samples under triaxial compression," *Journal of Mining Science*, vol. 41, no. 1, pp. 44–52, 2005.

[22] Y. Ju, L. Wang, H. Xie, G. Ma, Z. Zheng, and L. Mao, "Visualization and Transparentization of the Structure and Stress Field of Aggregated Geomaterials Through 3D Printing and Photoelastic Techniques," *Rock Mechanics and Rock Engineering*, vol. 50, no. 6, pp. 1383–1407, 2017.

[23] C. A. Tang and P. K. Kaiser, "Numerical simulation of cumulative damage and seismic energy release during brittle rock failure—part I: fundamentals," *International Journal of Rock Mechanics and Mining Sciences*, vol. 35, no. 2, pp. 113–121, 1998.

[24] X. Li, Z. Zhou, T.-S. Lok, L. Hong, and T. Yin, "Innovative testing technique of rock subjected to coupled static and dynamic loads," *International Journal of Rock Mechanics and Mining Sciences*, vol. 45, no. 5, pp. 739–748, 2008.

[25] B.-G. He, R. Zelig, Y. H. Hatzor, and X.-T. Feng, "Rockburst Generation in Discontinuous Rock Masses," *Rock Mechanics and Rock Engineering*, vol. 49, no. 10, pp. 4103–4124, 2016.